OFFICE OF NAVAL RESEARCH

Contract N00014-86-K-0556

Technical Report No. 70

Electrosorptive Detection Based on Double-Layer Capacitance for

Selective Anion Monitoring in Ion Chromatography.

I.   Mercury Electrodes

by

T. Ramstad and M. J. Weaver

Prepared for Publication

in the

Anal. Chim. Acta

Purdue University

Department of Chemistry

West Lafayette, Indiana 47907

September 25, 1987

AD-A188 780

REPORT DOCUMENTATION PAGE

1a REPORT SECURITY CLASSIFICATION	1b RESTRICTIVE MARKINGS
Unclassified	

2a SECURITY CLASSIFICATION AUTHORITY	3 DISTRIBUTION/AVAILABILITY OF REPORT
	Approved for public release and sale; its distribution is unlimited.
2b DECLASSIFICATION/DOWNGRADING SCHEDULE	

4 PERFORMING ORGANIZATION REPORT NUMBER(S)	5. MONITORING ORGANIZATION REPORT NUMBER(S)
Technical Report No. 70	

6a NAME OF PERFORMING ORGANIZATION	6b. OFFICE SYMBOL (if applicable)	7a NAME OF MONITORING ORGANIZATION
Purdue University Department of Chemistry		Division of Sponsored Programs Purdue Research Foundation

6c ADDRESS (City, State, and ZIP Code)	7b ADDRESS (City, State, and ZIP Code)
Purdue University Department of Chemistry West Lafayette, Indiana 47907	Purdue University West Lafayette, Indiana 47907

8a NAME OF FUNDING/SPONSORING ORGANIZATION	8b OFFICE SYMBOL (If applicable)	9 PROCUREMENT INSTRUMENT IDENTIFICATION NUMBER
Office of Naval Research		Contract No. N00014-86-K-0556

8c ADDRESS (City, State, and ZIP Code)	10 SOURCE OF FUNDING NUMBERS			
800 N. Quincy Street Arlington, VA 22217	PROGRAM ELEMENT NO	PROJECT NO	TASK NO	WORK UNIT ACCESSION NO

11 TITLE (Include Security Classification)
Electrosorptive Detection Based on Double-Layer Capacitance for Selective Anion Monitoring in Ion Chromatography. I. Mercury Electrodes

12 PERSONAL AUTHOR(S)
T. Ramstad and M. J. Weaver

13a TYPE OF REPORT	13b TIME COVERED	14 DATE OF REPORT (Year, Month, Day)	15 PAGE COUNT
Technical	FROM 10/1/86 TO 9/30/87	September 25, 1987	

16 SUPPLEMENTARY NOTATION

17	COSATI CODES		18 SUBJECT TERMS (Continue on reverse if necessary and identify by block number)
FIELD	GROUP	SUB-GROUP	hanging or dropping mercury electrode, liquid chromatography-double-layer capacitance (LC-DLC), large-volume wall-jet configuration

19 ABSTRACT (Continue on reverse if necessary and identify by block number)

A novel scheme is presented for the detection of selected anions in ion chromatography based on changes in differential double-layer capacitance, ΔC_d, for a metal electrode at a suitable electrode potential induced by specific anion adsorption. The detector in the liquid chromatography-double-layer capacitance (LC-DLC) arrangement described here is a hanging or dropping mercury electrode in a large-volume wall-jet configuration. The aqueous-phase anions observed to readily be detected using this approach include chloride, bromide, iodide, azide, thiocyanate, and thiosulfate. The ΔC_d-analyte concentration relationship can be arranged to be approximately linear at least over the range 1-100 ppm. A welcome feature of the technique is its insensitivity to ionic concentration gradients in the flowing stream. Another virtue of LC-DLC is its selectivity, although it is less sensitive for the detection of complexing anions in comparison with faradaic electrochemical detection (FEC) based on mercury oxidation. Dual detection schemes were also devised, involving DLC monitoring at two potentials or DLC combined with faradaic electrochemical detection.

20 DISTRIBUTION/AVAILABILITY OF ABSTRACT	21 ABSTRACT SECURITY CLASSIFICATION
☐ UNCLASSIFIED/UNLIMITED ☒ SAME AS RPT ☐ DTIC USERS	Unclassified

22a NAME OF RESPONSIBLE INDIVIDUAL	22b TELEPHONE (Include Area Code)	22c OFFICE SYMBOL

DD FORM 1473, 84 MAR
83 APR edition may be used until exhausted
All other editions are obsolete

ELECTROSORPTIVE DETECTION BASED ON DOUBLE-LAYER CAPACITANCE FOR

SELECTIVE ANION MONITORING IN ION CHROMATOGRAPHY.

I. MERCURY ELECTRODES

Tore Ramstad and Michael J. Weaver

Department of Chemistry

Purdue University, West Lafayette, IN 47907

ABSTRACT

A novel scheme is presented for the detection of selected anions in ion chromatography based on changes in differential double-layer capacitance, ΔC_d, for a metal electrode at a suitable electrode potential induced by specific anion adsorption. The detector in the liquid chromatography-double-layer capacitance (LC-DLC) arrangement described here is a hanging or dropping mercury electrode in a large-volume wall-jet configuration. The aqueous-phase anions observed to readily be detected using this approach include chloride, bromide, iodide, azide, thiocyanate, and thiosulfate. The ΔC_d-analyte concentration relationship can be arranged to be approximately linear at least over the range 1-100 ppm. A welcome feature of the technique is its insensitivity to ionic concentration gradients in the flowing stream. Another virtue of LC-DLC is its selectivity, although it is less sensitive for the detection of complexing anions in comparison with faradaic electrochemical detection (FEC) based on mercury oxidation. Dual detection schemes were also devised, involving DLC monitoring at two potentials or DLC combined with faradaic electrochemical detection.

INTRODUCTION

Ion chromatography (IC) has flourished as an analytical technique since the pioneering work of Small et al. in 1975 [1]. It has emerged as a mature, and extensively commercialized approach. Conductometry prevails as the predominant detection technique, applied to both suppressor- and single-column systems [2, 3]. An alternate universal scheme that is gaining acceptance is indirect photometric monitoring, a technique that relies on a decrease in absorbance as an eluting analyte dilutes the concentration of a designed photometric carrier in the eluent [4-6]. In contrast to these universal schemes, faradaic electrochemical detection (FEC) has found some use for selected anions, among them chloride, bromide, iodide, cyanide, thiocyanate, thiosulfate, and sulfide [7].

A different approach to *selective* electrochemical detection in ion chromatography which we introduce relies on changes in the double-layer capacitance of metal electrodes brought about by specific adsorption of an analyte [8, 9]. This approach, which we shall label "double-layer capacitance" (DLC) detection, involves the determination of the differential capacitance, C_d, at a suitable electrode by means of a.c. impedance measurements.

Several related analytical schemes have been described in the literature [8-15]. These techniques, commonly labeled "tensammetry", have generally involved the measurement of nonfaradaic currents at the mercury electrode associated with analyte adsorption. Tensammetry was actively investigated as a standalone analytical technique for organic surface-active agents some time ago [8, 9], but has been in a less active state in recent years. Despite its relatively selective nature, it is its lack of

discriminatory power where several surface-active agents compete that has limited its general utility.

One obvious approach to circumventing this limitation is to employ tensammetry together with liquid chromatography. The attractiveness of the approach relative to classical tensammetry derives in part from its sensitivity as a result of the ability to detect small transient changes in C_d resulting from passage of the analyte past the electrode detector in the chromatographic flow system. The union of such "electrosorption" analysis (ES) with LC (or IC) we will refer to as LC-ES (or IC-ES). A few attempts at combining LC and ES have been reported for surface-active organic analytes [10-15]. One potential area of application of such schemes is to the detection of inorganic anions, especially since anion -specific adsorption is often strongly dependent on the electrode potential and can yield large increases in C_d. We herein report on a coupled liquid chromatography-double-layer capacitance (LC-DLC) scheme for the selective detection of inorganic anions, employing either a hanging or dropping mercury electrode in a wall-jet configuration.

EXPERIMENTAL

Instrumentation

A phase-sensitive detection arrangement was used to measure the potential-dependent differential double-layer capacitance, C_d, at the hanging mercury drop electrode (HMDE). In this scheme, the potential applied by either a Princeton Applied Research (PAR) 173 or 273 potentiostat is modulated by a sinusoid of approximately 10 mV peak-to-peak amplitude and of frequency 50-400 Hz. The alternating portion of the cell

current is separated into its in-phase and out-of-phase (quadrature) components using a PAR Model 5204 lock-in amplifier; these in turn are directed to a computer (DEC PDP-11/23) which calculates the capacitance according to $C_d = (\omega E)^{-1}[(I_{out}^2 + I_{in}^2)/I_{out}]$, where ω is the ac frequency in radians s^{-1}, E is the magnitude of the sinusoid, and I_{in} and I_{out} are the magnitudes of the in-phase and out-of-phase components, respectively, of the cell current. The required changes in C_d, ΔC_d, are registered by applying the offset output of a DAC to a strip chart recorder.

The arrangement for use with a dropping mercury electrode (DME) is slightly more complicated and is shown in Figure 1; in this scheme, C_d is measured momentarily near the end of drop lifetime. Synchronization of the drop knocker and measurement circuitry is under the control of drop knocker logic circuitry. The drop knocker, track & hold amplifier, and low-pass filter/d.c. amplifier/slave track & hold amplifier were designed and constructed in-house [16]. The low-pass filter/d.c. amplifier allows for simultaneous amperometric (FEC) detection (*vide infra*).

Cell and Electrode Arrangement

To most readily accommodate the HMDE and DME without introducing the likely complications brought on by the miniaturization requirements of a thin-layer device, a design based on the wall-jet configuration in a large-volume electrochemical cell [17] was chosen. A Metrohm hanging mercury drop electrode (Model EA 410, Brinkmann Instruments Co.) was fitted in a custom-fabricated holder and cell assembly as shown in the inset to Figure 2. The glass capillaries (Brinkmann) were tapered as shown. The counter electrode was a coiled # 20-gauge Pt wire. An Ag/AgCl electrode filled

with 3M NaCl (Model RE-1, Bioanalytical Systems) served as the reference electrode. Connection between the cell and the LC column was made with 1/16" x 0.010" s.s. tubing.

The cell arrangement for the DME also is shown in Figure 2. The capillaries, of nominal 6 mm o.d. and 8" length, were either 0.004" or 0.005" i.d. (Wilmad Glass Co., Inc.). The tips were tapered as for the HMDE capillaries. Use of the Teflon or nylon fittings shown in the figure made for convenient assembly. An on/off valve (2-way miniature Teflon solenoid valve, 24V, P/N 2-32-020-2, General Valve Corporation) controlled the flow of mercury from a reservoir of variable height. Electrical connection was achieved through a # 16-gauge Pt wire epoxied into the Teflon union. Drop dislodgement was under the control of a Teflon-tipped, short-stroke (0.060") solenoid (Model 124910-031, Ledex Inc.) fitted with a return spring washer. Drop times of one or two seconds were generally employed.

The electrochemical cell is shown in partial view in Figure 2. Together with the electrode assembly described above, the geometry is that of the large-vessel wall-jet [17, 18]. The cell consists of a reference electrode arm, a three-way stopcock for deaeration and N_2 blanketing, an overflow tube, a mercury drawoff, an electrolyte "make-up" line, and a water jacket. The volume of the cell accessible to solution (i.e., with the Teflon holder assembly in place) is ca. 160 mL. The make-up line allows for continuous delivery via a syringe pump of a high concentration of a suitable salt solution to maintain a concentration of supporting electrolyte in the vessel appropriate to the requirements of electrochemistry. During use the cell was tilted at approximately 15° from

vertical to prevent mercury from clogging the lower capillary (eluent delivery nozzle). To assure isolation from electrical interference, the cell/electrode assembly was housed in a Faraday cage.

LC Equipment and Methods

All chromatography was conducted with aqueous eluents. Deionized water was further purified by passage through a "Milli-Q" water purification system (Millipore Corp.). The mobile phase usually consisted of dilute solutions of sodium perchlorate (vide infra), blanketed under nitrogen. The initial cell contents and make-up solutions were also deaerated under nitrogen flow, and all critical lines were constructed of stainless steel. As a further combatant to oxygen, the nitrogen source was followed by an Oxy-Trap (Alltech Associates, Inc.) and a BASF R3-11 catalytic oxygen scrubber; these were followed by a sparging vessel to saturate the carrier stream with water prior to entering the electrochemical cell.

Solvent delivery was under the control of a Waters Model 6000A pump (Waters Associates). Injections were made with a Rheodyne 710 injection valve (Rheodyne Incorporated), most often with a 50-μL sample loop. Two ion chromatography columns were used in this work: either a Vydac Ion Chromatography column (No. 302-IC46, The Separations Group), which consists of pellicular, silica-based packing, or a Hamilton PRP-X100 Ion Chromatography column, which contains resin-based anion exchange packing. The exchange capacity of the former is about 0.1 meq/g (dry) [19], while for the latter it is 0.17 meq/g [20]. Vydac SC pellicular packing was used as guard material with the Vydac packing, and Hamilton PRP-1 packing with

the PRP-X100.

To achieve electrosorptive detection in ion chromatography, a background (displacer) ion is required that exhibits little tendency to be specifically adsorbed. Fluoride is in principle the most suitable anion on this basis, with the oxyanions perchlorate, nitrate, and sulfate displaying weak, yet increasingly more significant specific adsorption [21, 22]. However, there are serious drawbacks to the use of fluoride in an LC system including its tendency to attack silica and pumping systems, and its inability to be employed in acid media. Another important consideration is that fluoride is an extremely weak displacer ion, and as such would likely lead to poorly shaped peaks.

Perchlorate suffers from none of these disadvantages. Our eluent of choice therefore contains sodium perchlorate, with perchloric acid added where acidic eluents are desired and either sodium or potassium hydroxide added where alkaline solutions are sought. Both hydronium and hydroxyl ions exhibit negligible specific adsorption at mercury [23]. If a higher concentration of electrolyte is desired, the more weakly displacing nitrate may be used. Additionally, judiciously chosen buffers may be used. For example, we have successfully used eluents containing a mixture of sodium perchlorate and 0.05 ionic strength buffers containing phosphate, formate, or acetate.

BACKGROUND AND RATIONALE

The fundamental premise on which the analytical utility of the technique described here is based is that a specifically adsorbing analyte of known bulk concentration will yield a corresponding coverage of adsorbed

analyte at an electrode poised at a suitable potential. This in turn yields a corresponding change in the differential capacitance, ΔC_d, with respect to the value, C_d, in the absence of analyte. The quantitative analytical utility of this detector clearly depends on the ability to relate the measured ΔC_d values to the bulk analyte concentration. A relationship between ΔC_d and bulk concentration can be formulated on the basis of surface thermodynamics, as follows.

The effect of specific adsorption of X on C_d at a given electrode potential, E, arising from the addition of a given bulk concentration of X, c_x, at a fixed ionic strength can be deduced starting from the cross-differential relationship [24]

$$\left(\frac{\partial q^m}{\partial \Gamma_x}\right)_E = -RT\left(\frac{\partial \ln c_x}{\partial E}\right)_{\Gamma_x} \tag{1}$$

where Γ_x is the surface concentration of specifically adsorbed X, q^m is the surface electronic charge density, and R and T have their usual meaning. For simplicity, let us assume that the differential coefficients in Eqn. 1 are independent of Γ_x and E. (This condition is approximated for a number of adsorbed anions [24].) Thus we can rewrite Eqn. 1 as

$$\left(\frac{\Delta q^m}{\Delta \Gamma_x}\right)_E = -RT\left(\frac{\Delta \ln c_x}{\Delta E}\right)_{\Gamma_x} \tag{1a}$$

It is also worth noting that the r.h.s. of Eqn. 1 can be identified with the potential dependence of the adsorption free energy, ΔG°_{ad} [24]:

$$-RT\left(\frac{\partial \ln c_x}{\partial E}\right)_{\Gamma_x} = \left(\frac{\partial \Delta G^\circ_{ad}}{\partial E}\right)_{\Gamma_x} \tag{2}$$

For anions, $\Delta G^\bullet_{ad}$ will commonly be strongly dependent upon E such that shifting the potential negative will increase ΔG°_{ad} so to incur eventual complete desorption. Since we are concerned here with total capacitance changes induced by the presence of adsorbate, it is useful to define the overall change in q^m, Δq^m_t, induced for a given electrode potential by the addition of the adsorbate. From the form of Eqn. 1a, anion adsorption will yield positive Δq^m_t values that increase for a given c_x value as the potential becomes more positive. The corresponding increase in C_d at a given potential caused by specific adsorption, ΔC_d, can be related to Δq^m_t by

$$\Delta C_d = \left(\frac{\partial \Delta q^m_t}{\partial E}\right)_{c_x} \tag{3}$$

Provided that the variation in Γ_x is linear in c_x (i.e., the adsorption isotherm follows Henry's Law at constant E), since Δq^m is proportional to $\Delta\Gamma_x$ (Eqn. 1a), Δq^m_t will also be proportional to c_x. From the assumed constancy of the coefficient $(\partial \ln c_x/\partial E)_{\Gamma_x}$ in Eqn. 1 and noting that under Henry's Law conditions $(\partial \ln c_x/\partial E)_{\Gamma_x} = -(\partial \ln \Gamma_x/\partial E)_{c_x}$, we also expect that $(\partial\Gamma_x/\partial E)_{c_x}$ and therefore $(\partial\Delta q^m_t/\partial E)_{c_x}$ will be proportional to Γ_x and hence to c_x. In view of Eqn. 3, we deduce that at a given electrode potential under these conditions

$$\Delta C_d = K\Gamma_x \tag{4}$$

and $\Delta C_d = K'c_x$ $\tag{4a}$

where the magnitude of the coefficient K will be related to the extent of the potential dependence of $\Delta G^{\bullet}_{ad}$, and that of K' additionally to the absolute value of $\Delta G^{\bullet}_{ad}$.

This analysis implies that two factors are desirable for the quantitative detection of an adsorbing species via increases in C_d: (1) the presence of a linear adsorption isotherm, and (2) strongly potential-dependent adsorption. Although not in itself limited to anions, the latter requirement together with the need for favorable adsorption thermodynamics makes the approach most applicable to this class of adsorbates.[*] A clearly important question is the extent of the surface coverage region over which the adsorption isotherm retains at least rough obeyance to Henry's Law; large deviations even at moderate coverages are well known and attributed to repulsive anion-anion interactions.

Figures 3a and 3b contain two illustrative examinations of this matter, using published data for adsorbed iodide at mercury in mixed potassium fluoride/potassium iodide media having a constant unit ionic strength [25]. Plots are presented for both Δq^{m}_{t} (open squares) and ΔC_d (closed circles) versus c_x for solution iodide for E = -0.70 V (Fig. 3a), and E = -1.00 V (Fig. 3b). In view of the proportionality between Δq^{m}_{t} and Γ_x (vide supra), the Δq^{m}_{t}-c_x plot is tantamount to an adsorption isotherm. (The Y-axis scales are arranged so to yield equal slopes for these pairs of plots at low iodide coverages.) It is seen that both the Δq^{m}_{t} and ΔC_d

---

[*] For organic adsorbates, in particular, the decreases in capacitance commonly seen upon adsorption can be attributed primarily to changes in the dielectric properties of the inner layer; the variations in adsorption free energy with potential are typically milder for these systems than for charged adsorbates.

plots in Figure 3a are linear over the region $\Delta C_d \leq 10 \ \mu F \ cm^{-2}$, which corresponds to $\Gamma_x \leq 7 \times 10^{-12} \ mol \ cm^{-2}$; and in Figure 3b for $\Delta C_d \leq 7 \ \mu F \ cm^{-2}$, which corresponds to $\Gamma_x \leq 5 \times 10^{-12} \ mol \ cm^{-2}$. At higher coverages, both pairs of plots exhibit decreasing slopes, consistent with repulsive adsorbate-adsorbate interactions. Note that similar ΔC_d values yet differing c_x values correspond to the linear isotherm region for these two potentials, as expected in view of the strongly potential-dependent adsorption. The same treatment applied to published data for chloride [26], bromide [27], and azide [28] also yields similar results.

At least at mercury electrodes, comprehensive detailed information is available on the thermodynamics of anion adsorption. The strength of adsorption can be related to several factors, including electrostatic and covalent interactions and the loss of hydration energy [29]. Extensive specific adsorption is observed for a wide range of anions, including oxyanions as well as halides and pseudohalides [23]. However, the strength of adsorption varies substantially, being greatest for polarizable coordinating anions (e.g., iodide, thiocyanate) [23].

This information therefore suggests that DLC detection should provide a *selective* as well as *sensitive* analytical probe for anion solutes. One obvious strategy is to select an electrode potential so as to yield the desired detection sensitivity for a given anion, preferably also so to provide a linear ΔC_d-c_x response and minimal interference from other anions.

RESULTS AND DISCUSSION

We present here our findings on the utility of IC-DLC. Anions

yielding measurable ΔC_d responses at analytically useful concentration levels are detailed and their ΔC_d-c_x response curves presented and discussed. Since the wall-jet cell/electrode geometry employed here is somewhat unconventional, optimization studies for this detector are also noted. Some special features of electrosorptive detection at mercury are highlighted, including gradient compatibility and alternate drop, dual-potential detection.

Identification of Anions suitable for LC-DLC

Published C_d-E curves obtained for fundamental examinations of specific ion adsorption may be consulted as an aid in predicting expected changes in capacitance upon specific adsorption for the present purposes. However, the bulk concentrations usually employed in the former studies are higher than those employed in modern ion chromatography so that such plots are not necessarily reliable indicators of the relative changes in capacitance to be expected under the conditions required for the present application. Furthermore, capacitance-potential information is not available for a number of ions of interest in ion chromatography. Therefore, in the present study, we have examined systematically this fundamental feature for most anions of common interest in IC.

Table 1 lists the anions investigated by us. Of these, six were ascertained to be detectable by DLC at concentrations competitive with conductometric and indirect photometric detection; they are chloride, bromide, iodide, thiocyanate, thiosulfate and azide. Anticipated, but missing from this list, is cyanide, whose elution proved unsatisfactory under the eluent/column conditions employed in this study. For each of

these ions a plot of capacitance change (ΔC_d) vs. electrode potential was generated by IC-DLC; the curves for the halides shown in Figure 4 are illustrative. Such curves may be used as an aid in selecting appropriate potentials for analysis. A separation of these six electrosorptive ions with DLC detection is shown in Figure 5. Note the changes in potential made during the run, illustrating how the selectivity as well as sensitivity may be tailored to the needs of a particular analysis.

Calibration curves of normalized capacitance response, $\Delta C_d/C_d$, against analyte concentration were generated for the six tensioactive ions at several potentials at concentrations ranging from the limit of detection (ca. 0.2-0.5 ppm) to ca. 200 ppm. The bulk of the measurements were made using the HMDE; a few runs were rechecked using the DME. Most experiments employed the Vydac chromatographic column.

Representative calibration curves for bromide obtained at four potentials between -0.30 and -0.15 V at the HMDE are presented in Figure 6. Deviations from linearity for the $\Delta C_d/C_d$-concentration plots are seen only for the least negative potential, where the extent of specific adsorption is the greatest.

As expected, then, the response curves shown in Figure 6 show a general concordance with Figures 3a and b. At concentrations higher than those shown in Figure 6, the $\Delta C_d/C_d$-concentration curves exhibit increasingly nonlinear behavior as also observed in Figure 3. However, the linear or nearly-linear region of the response curves may be extended to larger analyte concentrations simply by shifting the potential to a more negative value. However, these higher concentrations are generally beyond those of typical interest in ion chromatography. At higher concentrations

DLC detection could, presumably, be extended to many additional anions, since virtually all anions specifically adsorb to a certain extent (29). However, to accommodate these higher concentrations, conventional ion-exchange columns would have to be employed.

Detector Optimization

As a first step in assessing the characteristics of DLC detection in the large-volume wall-jet configuration, detector performance was evaluated as a function of several parameters. Varying the separation between the mercury capillary and the eluent delivery nozzle (Figure 2) showed the expected increase in response (ΔC_d) as the separation was made smaller, although with a corresponding increase in baseline noise. As would be expected, increased noise was most apparent at the lowest eluent electrolyte concentrations. A welcome characteristic of the large-volume wall-jet configuration is that the peak detection efficiency is retained over a considerable nozzle-electrode separation (*vide infra*). Within limits, a decreased response at greater separation distances can be compensated for by increasing the gain through the system. A generally satisfactory separation was found to be about twice the diameter of the mercury drop, whether in the HMDE or DME configuration.

For some time, a *modus operandi* held that cell volumes in LC-FEC must be miniaturized to avoid the introduction of extra-column band broadening effects. This is now recognized not to be necessary in the large-volume wall-jet geometry [30-32]. Attributes of this geometry noted in the present work include generally simplified handling, avoidance of problems with mercury clogging that can plague thin-layer cells, and minimization of

dead-volume effects.

As noted above, a further benefit to the wall-jet geometry that we have observed is that virtually any desired supporting electrolyte condition can be achieved by introducing a suitable make-up stream without the band spreading or dilutive effect which may be introduced by post-column additions via a tee. Additionally, the capillary-delivery nozzle separation can be adjusted as mobile phase conditions dictate. For example, when using low displacer ion concentrations (a few millimolar), as is required to achieve retention of early eluting ions on the low-capacity Vydac chromatography column, the nozzle-electrode separation may be increased so as to enhance the contribution of the make-up stream to the overall electrolyte concentration and to lessen the contribution of the eluent stream; the net effect of this is to increase the average electrolyte concentration that is sensed by the electrode detector.

The minimum absolute detectable change in capacitance depends on the mercury drop size, and hence the electrode area. However, the smallest relative change that can be sensed with a signal-to-noise of 2.5 is about 1 part in 250. For an absolute capacitance of 2.5×10^{-7} F (typical), this corresponds to a change of 1×10^{-9} F. Concentrations on the order of 0.2-0.5 ppm (50 μL loop) are required to effect relative changes of this magnitude; these concentrations are comparable to detection limits usually quoted for conductometric and indirect photometric detection [33].

A number of other parameters besides capillary separation have an effect on system performance. Among these are the a.c. frequency and amplitude just as in conventional a.c. impedance measurements. Most experiments in the present work employed the frequency range 90-250 Hz. As

anticipated, the response increases, as does the noise, with both frequency and magnitude of the modulating sinewave. The most suitable a.c. frequency and amplitude values were found to be 90-145 Hz and 10 mV peak-to-peak, respectively. A prefilter setting of 0.1 s and a time constant up to 0.3 s on the lock-in amplifier were found appropriate with the HMDE; somewhat greater signal filtering was required with the DME.

Detection with Simultaneous Amperometric Readout

Allusion was made above to the benefit afforded by simultaneously evaluating the d.c. faradaic current record. Thus the capacitance measurements themselves are only valid in the absence of faradaic current arising from reversible redox processes. In the presence of such currents, large apparent increases in the measured capacitance can be obtained that in actuality arise from faradaic rather than capacitive (i.e., nonfaradaic) currents. The demonstrated absence of significant d.c. currents under the conditions where the capacitance response is being monitored provides a confirmation that the latter measurements are indeed valid.

The merit of such a scheme is exemplified in Figure 7, which shows dual "apparent capacitance" and FEC (amperometric) traces for sulfide. In this case, had only the capacitance output been monitored, the observed signal would erroneously have been interpreted as being due solely to analyte adsorption, whereas in fact, as is evident from the lower trace, the signal arises, at least in part, from sulfide-induced oxidation of mercury.

Gradient Elution in IC-DLC

Gradient elution has for a long time proven vexing in ion chromatography, although recently a solution was advanced which places a fiber suppressor column after the separating column [34, 35]. Single-column IC, though, has proven extremely recalcitrant to continuous gradient elution with conductivity detection. Double-layer capacitance detection is better suited for gradient analysis since, in comparison tc ionic conductivity, the former is relatively insensitive to ionic strength for nonadsorbing ions [36].

To illustrate this point, we performed a gradient experiment in which two pumps fed a pre-column mixing chamber. One feed consisted of 2.5×10^{-3} M sodium perchlorate and the other of 2.0×10^{-2} M sodium perchlorate. The gradient program is given in the legend of Figure 8, which shows the DLC chromatogram of a gradient separation of four ions. Over the concentration change brought about by this particular gradient program, C_d increases by 35%. The equivalent run with conductivity detection would not be practical, as the background conductance is estimated to increase by 470%.

Dual Capacitive and Capacitive-Amperometric Detection

Up to this point we have restricted DLC detection to single-potential monitoring, although an example has been given where the potential has been altered during a chromatographic analysis where several different anions are eluted (Fig. 5). The virtues of dual (two working) electrode detection in LC-FEC have been demonstrated recently [37, 38]. At least two benefits accrue: (1) enhanced selectivity, and (2) an aid to species

identification. The latter can be gleaned through a comparison of the ratio of amperometric currents obtained at two potentials with the expected ratio based on a previously generated voltammogram for the species in question. More exotic schemes such as combined amperometric-voltammetric detection have also been explored recently [39]. In a similar vein, and for identical reasons, DLC responses may be compared at two potentials, although at a greater cost in complexity than in conventional faradaic electrochemical detection.

Figure 9 presents the arrangement used here for alternate drop, dual-potential DLC detection. The two track & hold amplifiers are triggered on alternate drops, and hence each monitors the capacitance at a different potential. The potential program was generated by a PAR 175 Universal Programmer. The dual chromatograms shown in Figure 10 illustrate the complementary information that can be obtained with this scheme. Comparison of Figure 10 with Figure 5, which was obtained under nearly identical conditions, reveals, however, the greater baseline noise produced in the dual-potential mode.

An alternate two-potential experiment combines capacitance with amperometric detection. The only change required in the above instrumental arrangement is to switch the input line to one of the two track & hold amplifiers from the DAC (line 1 in Figure 9) to the output of the potentiostat (line 2). Alternate drop, dual-potential DLC-FEC detection should afford at least two benefits. First; as before, it should allow an assessment of compound purity by reference to the DLC and FEC response curves (ΔC_d-E for the former, Δi-E for the latter). Second, by providing two complementary views of a sample, different selectivities should obtain.

In general, we anticipate greater freedom from possible interferences in the ideally polarized region suitable for double-layer measurements. However, the detection limits appear to be significantly higher for DLC as compared with FEC methods for the systems considered here when the latter employ anion-induced mercury oxidation.

Figure 11 demonstrates combined DLC (a) and FEC (b) detection of chloride and bromide under conditions where the capacitance measurement potential was maintained constant at -0.20 V throughout all runs while the oxidative potential was incrementally increased from -0.30 V to +0.20 V, as indicated. The mechanically induced drop time was 1s. Comparison of the successive capacitance traces reveals the excellent reproducibility of the measurement in this rather complicated scheme (relative standard deviation of 5.1% for chloride, 4.0% for bromide). Note that the baseline noise for capacitance is of the same order of magnitude seen in the dual-potential capacitance runs of Figure 10. In the lower (oxidative) traces in Figure 11, we note that there is no response for bromide at -0.30 V, it is just evident at -0.20 V, and proceeds to shoot off scale at +0.20 V. Chloride is not detected in these traces until 0 V.

Capacitance Detection Using Thin-Layer Cells

As an alternative to the large-volume wall-jet, a thin-layer device incorporating a mercury electrode may also be used. We have constructed such a device incorporating a rapidly dropping mercury electrode. However, we defer discussion of it to a subsequent publication.

A related approach which we briefly investigated was to form a mercury amalgam on a suitable substrate, as is common in LC-FEC [40, 41]. The C-E

curves we obtained for a mercury film on gold revealed a relatively smaller polarizable potential range, especially in the positive direction where the limit was shifted negative by some 0.4-0.5 V relative to mercury. Since this does not bode well for amalgamated gold as a suitable surface for DLC detection, we did not pursue this approach.

Concluding Remarks

The foregoing describes a new means of detection based on electrosorption which we believe can have substantial utility for the selective determination of anions in ion chromatography. Detection relies on increases in differential capacitance induced by ions specifically adsorbed at an ideally polarized electrode. We have found a number of anions to be readily determinable using this LC-DLC approach at the concentrations generally of interest in contemporary ion chromatography. Their ΔC_d-bulk concentration response curves are satisfactorily linear over a sufficient range so to facilitate quantitative analysis using this approach. If higher analyte concentrations are of interest, virtually all common anions are determinable, at least when DLC detection is coupled to conventional (high-capacity) anion-exchange columns.

Detection is most conveniently achieved using the large-volume wall-jet design. A welcome feature of the technique is its tolerance of the presence of ionic concentration gradients. Dual information may be obtained by employing simultaneous capacitive-amperometric detection, alternate drop, dual-potential capacitive-capacitive detection, and alternate drop, dual-potential capacitive-amperometric detection.

We have also applied the DLC approach for detecting a variety of organic species in aqueous LC systems. In addition, we have also explored

the utility of silver as an electrode for such double-layer capacitance detection of aqueous-phase anions. Publications on these topics will be forthcoming.

REFERENCES

1 H. Small, T. S. Stevens and W. C. Bauman, Anal. Chem., 47 (1975) 1801.

2 J. S. Fritz, D. T. Gjerde and C. Pohlandt, Ion Chromatography, Dr. Alfred Huthig Verlag, Heidelberg, 1982.

3 F. C. Smith, Jr. and R. C. Chang, The Practice of Ion Chromatography, John Wiley and Sons, New York, 1982.

4 H. Small and T. E. Miller, Jr., Anal. Chem., 54 (1982) 462.

5 Z. Iskandarani and T. E. Miller, Jr., Anal. Chem., 57 (1985) 1591.

6 D. R. Jenke, Anal. Chem., 56 (1984) 2674.

7 R. D. Rocklin, J. Liq. Chromatogr., 2 (1984) 588.

8 H. Jehring, Elektrosorptionsanalyse mit der Wechselstrompolarographie, Akademie-Verlag, Berlin, 1974.

9 B. Breyer and A. H. Bauer, Alternating Current Polarography and Tensammetry, Volume XIII, Chemical Analysis, John Wiley, New York, 1963.

10 W. Kemula, B. Behr, K. Chlebicka and D. Sybilska, Roczniki Chem., 39 (1965) 1315.

11 Z. Borkowska, D. Sybilska and B. Behr, Roczniki Chem., 45 (1971) 269.

12 J. Laukelma and H. Poppe, J. Chromatogr. Sci., 14 (1976) 310.

13 W. Kemula and W. Kutner, J. Chromatogr., 204 (1981) 131.

14 H. G. de Jong, W. H. Voogt, P. Bos and R. W. Frei, J. Liq. Chromatogr., 6 (1983) 1745.

15 A. M. Bond and R. D. Jones, Anal. Chim. Acta, 152 (1983) 13.

16 T. Ramstad, Ph.D. Thesis, Purdue University, 1987.

17 S. K. Vohra, Am. Lab., 13(5) (1981) 66.

18 Zs. Niegreisz, L. Szucs, J. Fekete, G. Horvai, K. Toth and E. Pungor, J. Chromatogr., 316 (1984) 451.

19 R. E. Majors, J. Chromotogr. Sci., 15 (1977) 333.

20 D. P. Lee, J. Chromatogr. Sci., 22 (1984) 327.

21 P. Delahay, Double Layer and Electrode Kinetics, John Wiley and Sons, New York, 1965, Chapter 4.

22 R. Reeves, in J. O'M. Bockris, B. E. Conway and E. Yeager, (Ed.), Comprehensive Treatise of Electrochemistry, Vol. 1, Plenum Press, New York, 1980, Chapter 3.

23 M. A. Habib and J. O'M. Bockris, in J. O'M. Bockris, B. E. Conway and E. Yeager (Ed.), Comprehensive Treatise of Electrochemistry, Vol. 1, Plenum Press, New York, 1980, Chapter 4.

24 M. J. Weaver and F. C. Anson, J. Electroanal. Chem., 65 (1975), 737.

25 E. Dutkiewicz and R. Parsons, J. Electroanal. Chem., 11 (1966) 100.

26 R. Payne, Trans. Faraday Soc., 64 (1968) 1638.

27 A. R. Sears and P. A. Lyons, J. Electroanal. Chem., 42 (1973) 69.

28 E. R. Gonzales, J. Electroanal. Chem., 90 (1978) 431.

29 J. O'M. Bockris and A. K. N. Reddy, Modern Electrochemistry, Vol. 2, Plenum Press, New York, 1970, Chapter 7.

30 J. Yamada and H. Matsuda, J. Electroanal. Chem., 44 (1973) 189.

31 H. Gunasingham and B. Fleet, Anal. Chem., 55 (1983) 1409.

32 H. Gunasingham, Anal. Chim. Acta, 159 (1984) 139.

33 P. R. Haddad and A. L. Heckenberg, J. Chromatogr., 300 (1984) 357.

34 J. G. Tartar, Anal. Chem., 56 (1984) 1264.

35   J. S. Fritz, Anal. Chem., 59 (1987), 335A.

36   A. J. Bard and L. R. Faulkner, Electrochemical Methods, John Wiley and Sons, New York, 1980, p.488.

37   S. A. McClintock and W. C. Purdy, Anal. Chim. Acta, 148 (1983) 127.

38   J. Dutrien and Y. A. Delmotte, Fresenius Z. Anal. Chem., 314 (1983) 416.

39   C. E. Lunte, S.-W. Wong, T. H. Ridgway and W. R. Heineman, Anal. Chim. Acta, 188 (1986) 263.

40   K. Bratin, P. T. Kissinger and C. S. Bruntlett, J. Liq. Chromatogr., 4 (1981) 1777.

41   L. A. Allison and R. E. Shoup, Anal. Chem., 55 (1983) 8.

TABLE 1

Anions Investigated for Electrosorptive Activity

Cl^-	SO_3^{2-}	$S_2O_3^{2-}$	ClO^-	BrO_3^-	SiO_3^{2-}
Br^-	HS^-	HBO_4^{2-}	ClO_2^-	OCN^-	HCO_2^-
I^-	SO_4^{2-}	HPO_3^{2-}	ClO_3^-	N_3^-	
NO_2^-	SCN^-	$H_2PO_2^-$	IO_3^-	CrO_4^{2-}	
NO_3^-	CN^-	CO_3^{2-}	IO_4^-	$B_4O_7^{2-}$	

Figure 1

Block diagram of the instrumental arrangement for fixed-potential monitoring of double-layer capacitance at a DME with simultaneous faradaic electrochemical detection.

Figure 2

Large-volume wall-jet cell/electrode assembly for the DME used in IC-DLC detection. Inset: HMDE. See text for details.

Figure 3a

Plots of increase of differential double-layer capacitance, ΔC_d (closed circles), and the increase of the overall electrode charge density, Δq_t^m (open squares), induced by iodide specific adsorption at the mercury-aqueous interface against iodide solution concentration for fixed electrode potential of -0.70 V vs. SCE. Solution composition is $(1 - x)M\ KF + xM\ KI$. Extracted from experimental data in ref. 25.

Figure 3b

As for Fig. 3a, but for a fixed electrode potential of -1.00 V.

Figure 4

Relative changes in double-layer capacitance vs. potential at the HMDE for fixed concentrations of halide (100 ppm Cl^-, 50 ppm Br^-, 10 ppm I^-) determined by IC-DLC (100 ppm $Cl^- = 2.82$ mM, 50 ppm $Br^- = 0.62$ mM, 10 ppm $I^- = 0.079$ mM).

Figure 5

A separation of six ions with double-layer capacitance detection at the DME. Conditions: column, Hamilton PRP-X100; eluent, 1.2×10^{-2} M $NaClO_4$, pH 9.0 with NaOH; flow rate, 1.0 cm^3/min; initially in cell, 0.1 M NaF; make-up, 0.76 M NaF delivered at 0.13 cm^3/min; capillary, 0.004" i.d.; forced drop rate, 2 s/drop; delay, track & hold, 1.72 s; track time, 40 ms; sample composition: 100 ppm Cl^-, 100 ppm N_3^-, 50 ppm Br^-, 40 ppm I^-, 20 ppm $S_2O_3^{2-}$, and 80 ppm SCN^-.

<u>Figure 6</u>

Normalized calibration curves for Br⁻ at -0.30, -0.25, -0.20, and -0.15 V at the HMDE obtained on a Vydac column (100 ppm Br⁻ = 1.25 mM).

<u>Figure 7</u>

Simultaneous DME traces of capacitive and faradaic current for an injection of Na_2S; eluent, 0.8×10^{-2} M $NaClO_4$, pH 10.5 with NaOH. The upper trace (a) is the capacitive response while the lower (b) is the faradaic response.

<u>Figure 8</u>

A gradient separation of four ions with DLC detection. Conditions: column, Vydac; gradient solutions: <u>A</u> - 2.5×10^{-3} M $NaClO_4$, pH 4.9 with $HClO_4$; <u>B</u> - 2.0×10^{-2} M $NaClO_4$, pH 4.9 with $HClO_4$; gradient program, initially <u>A</u> at 1.4 cm^3/min, <u>B</u> switched in after 5 min at 0.9 cm^3/min, then <u>A</u> dropped back to 0.5 cm^3/min; potential, -0.25 V; sample composition: 200 ppm Cl⁻ (not detected), 100 ppm Br⁻, 5 ppm I⁻, 40 ppm SCN⁻, and 50 ppm $S_2O_3^{2-}$.

<u>Figure 9</u>

Block diagram of the instrumental arrangement for alternate drop, dual-potential capacitive-capacitive detection and alternate drop, dual-potential capacitive-amperometric detection. The track & hold input line marked 1 is for the former while 2 is for the latter.

<u>Figure 10</u>

Dual chromatograms obtained at two sets of potentials in alternate drop, dual-potential IC-DLC detection. Analysis conditions are nearly identical to those of Figure 5.
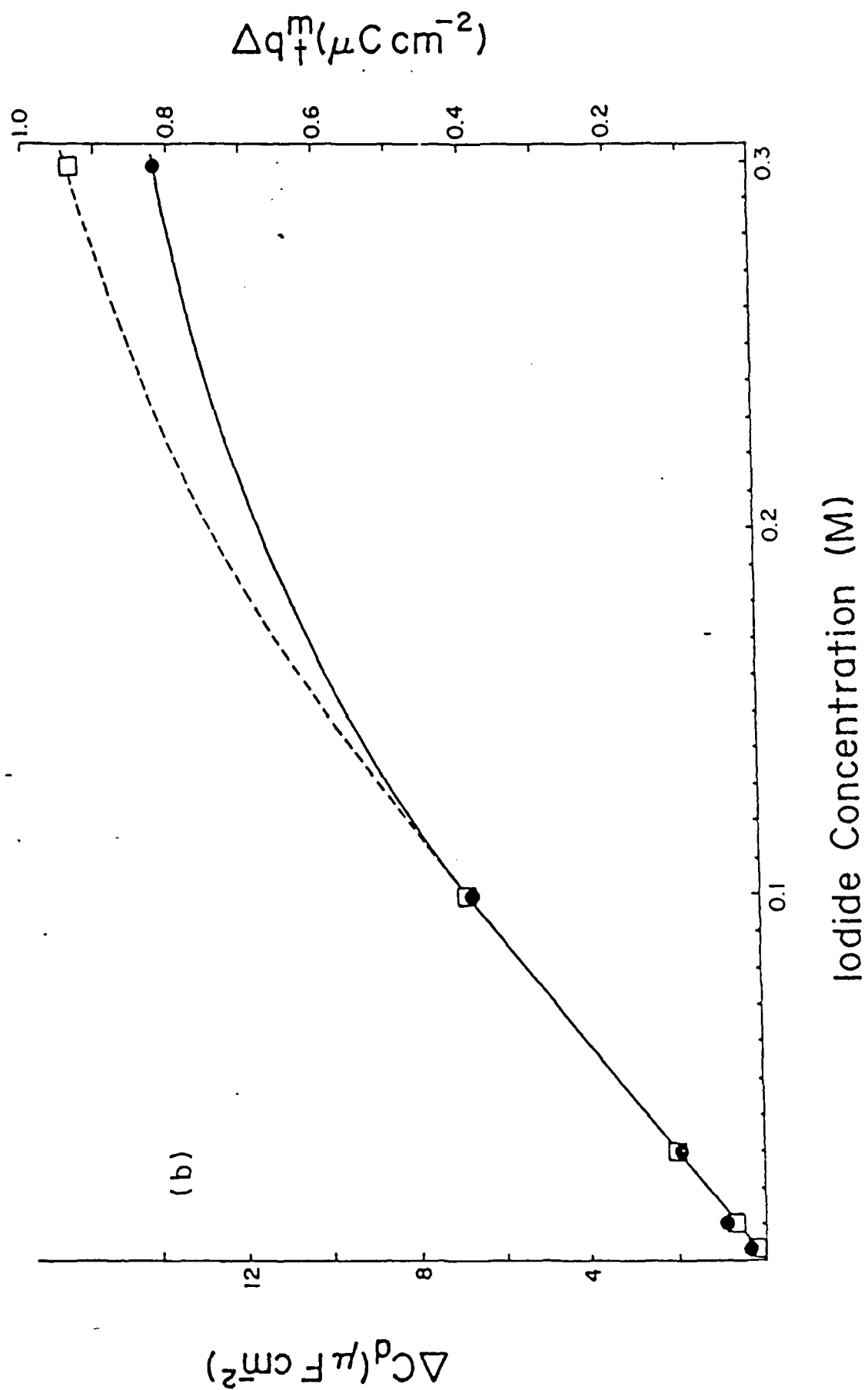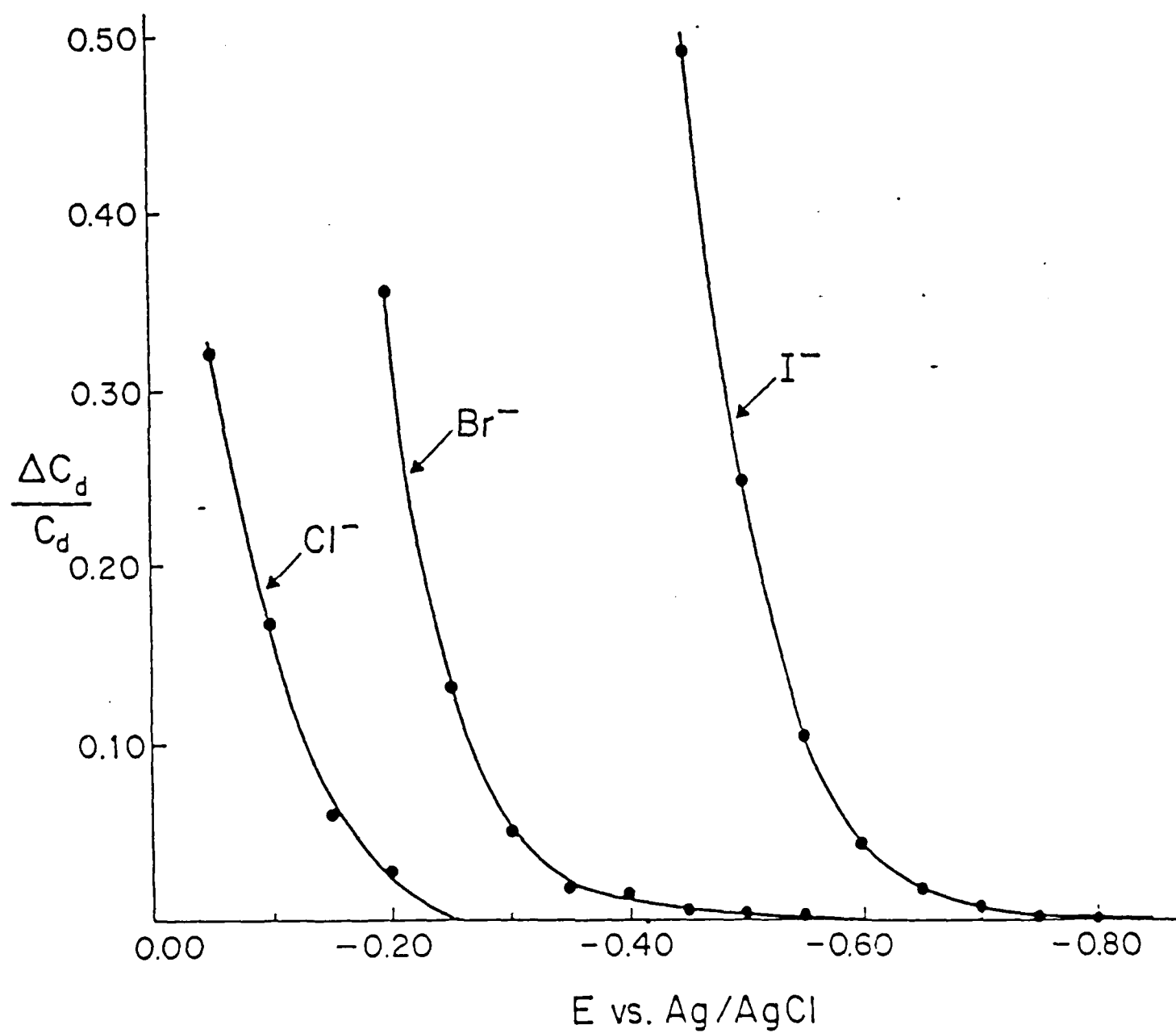
<u>Figure 11</u>

Dual chromatograms obtained by alternate drop, dual-potential capacitive-amperometric detection. Chromatographic conditions are identical to those in Figure 10. Sample composition: 200 ppm Cl⁻, 50 ppm Br⁻.
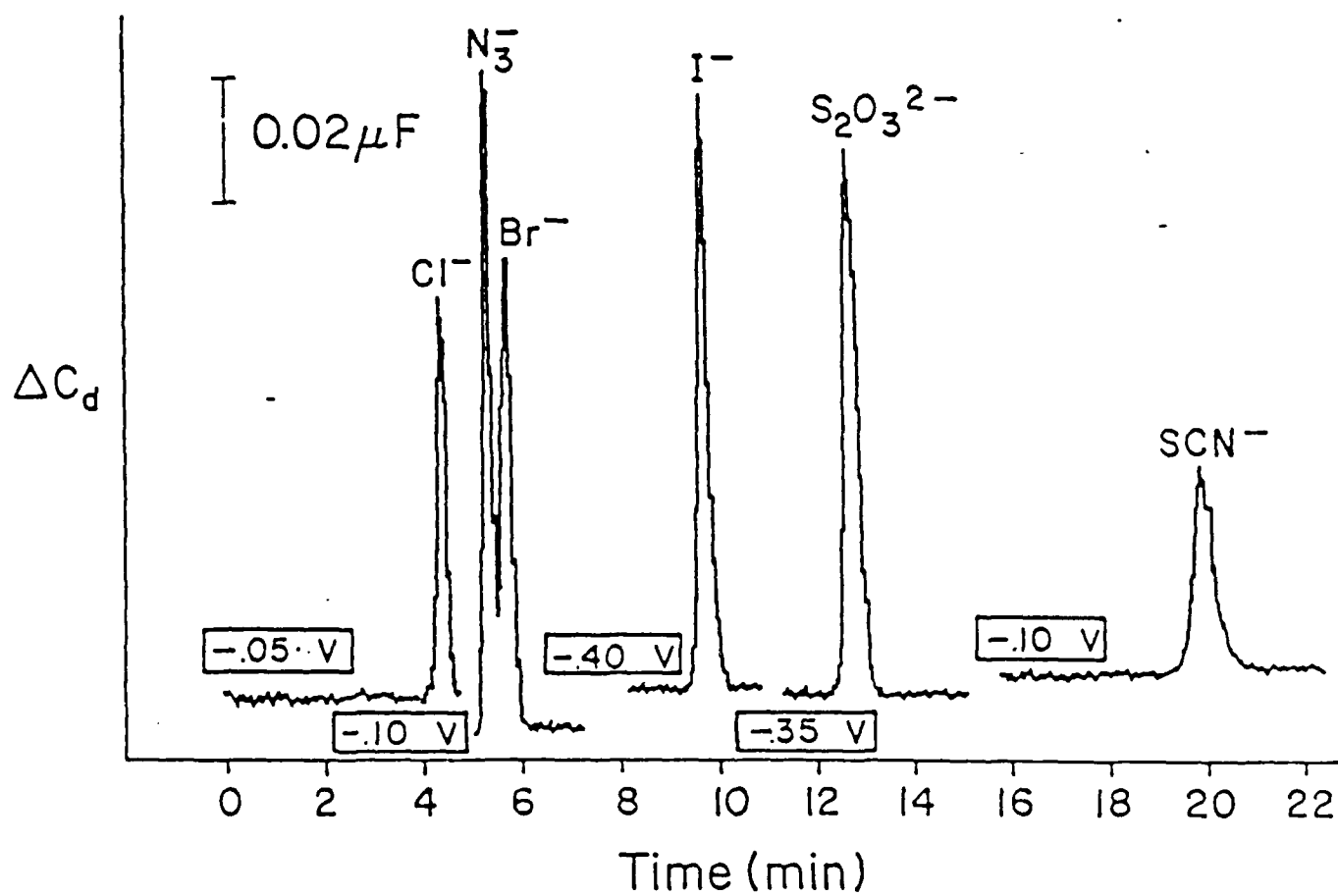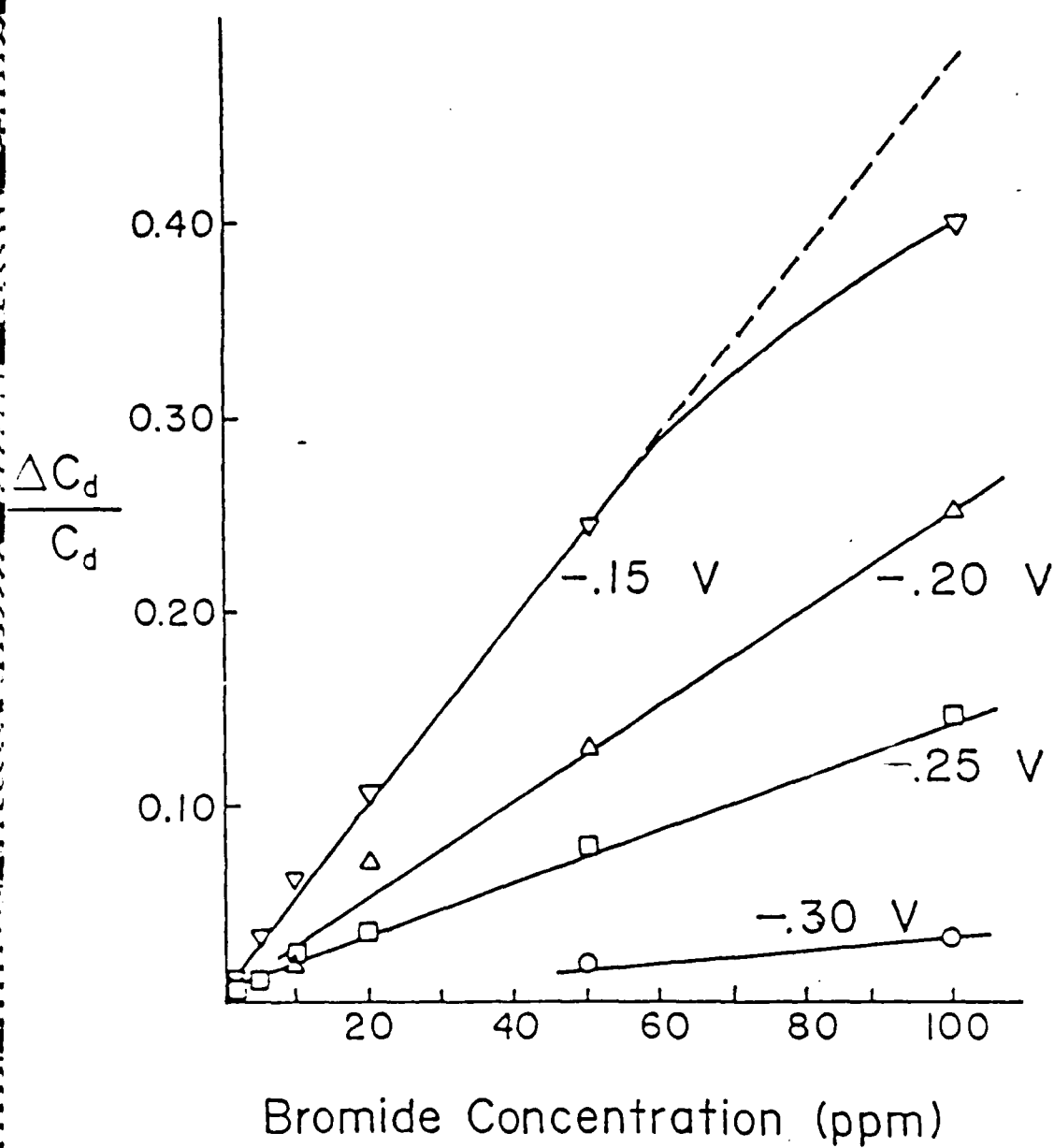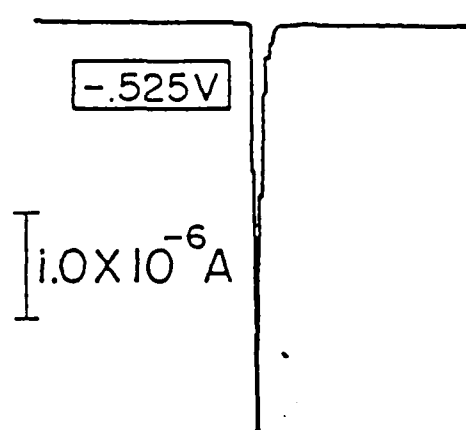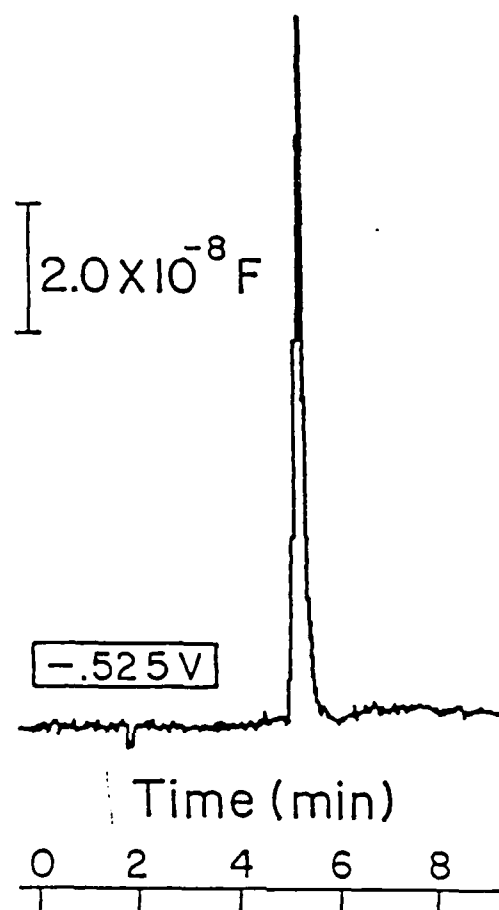
(a)

(b)

Bromide Concentration (ppm)

(a) DLC detection

2.0×10^{-8} F

$-.525$ V

Time (min)

0   2   4   6   8

$-.525$ V

1.0×10^{-6} A

(b) FEC detection

Upper trace labels (left to right): Cl⁻, N⁻, Br⁻, I, $S_2O_3^{2-}$, SCN⁻

Voltage boxes (upper): −.25 V, −.40 V, −.20 V

Voltage boxes (lower): −.10 V, −.30 V, −.10 V

X-axis (both traces): 0 2 4 6 8 10 12 14 16 18 20
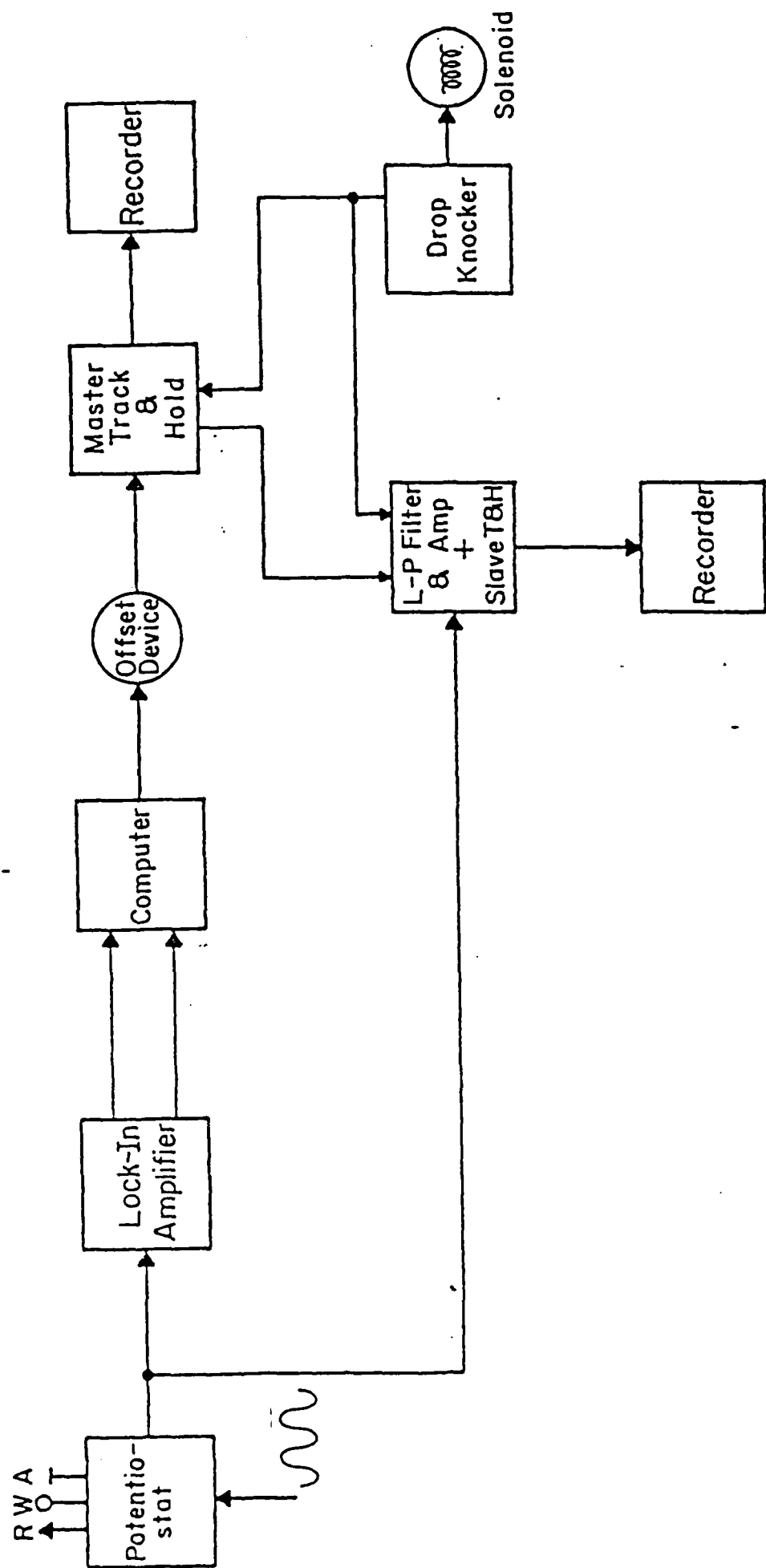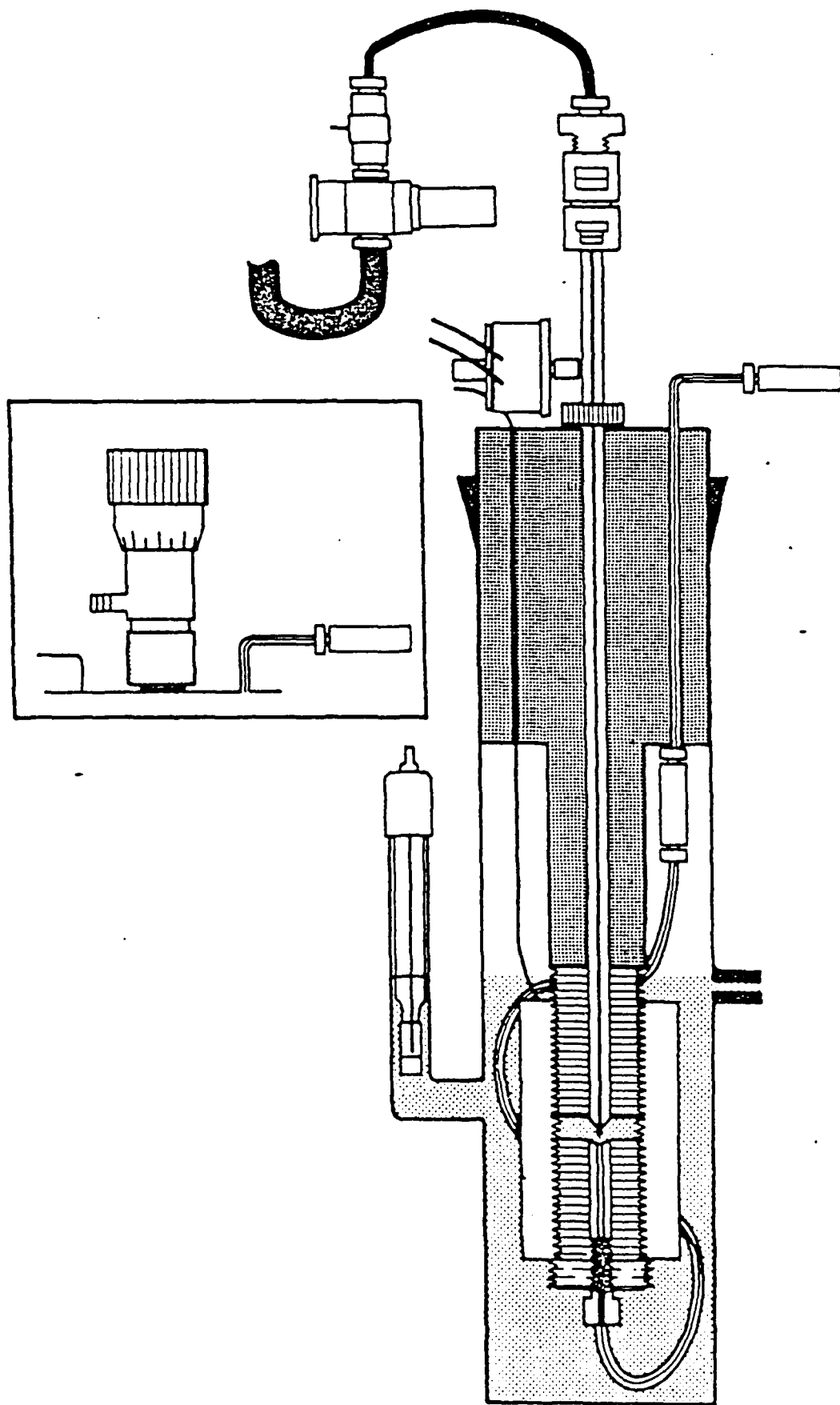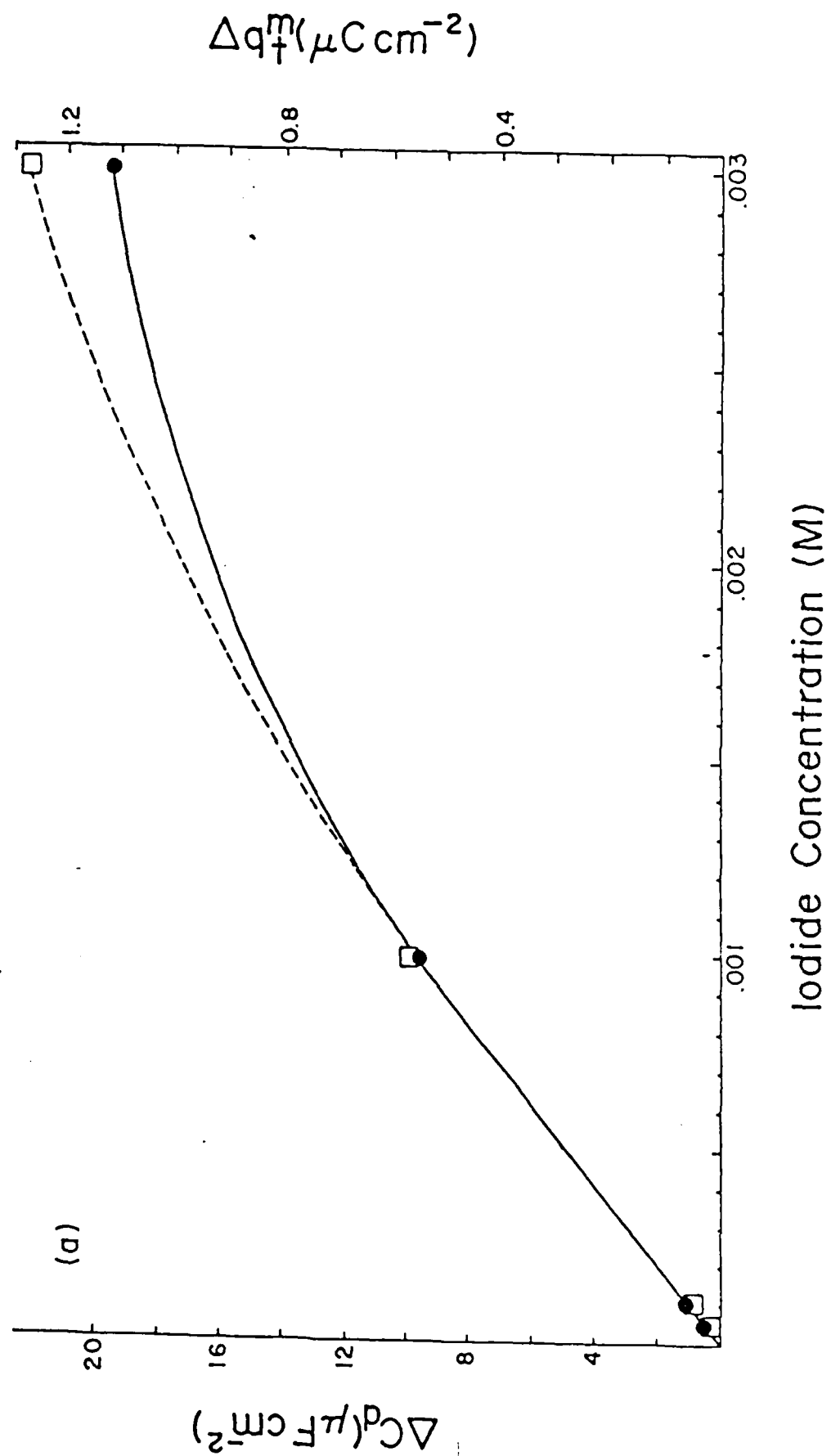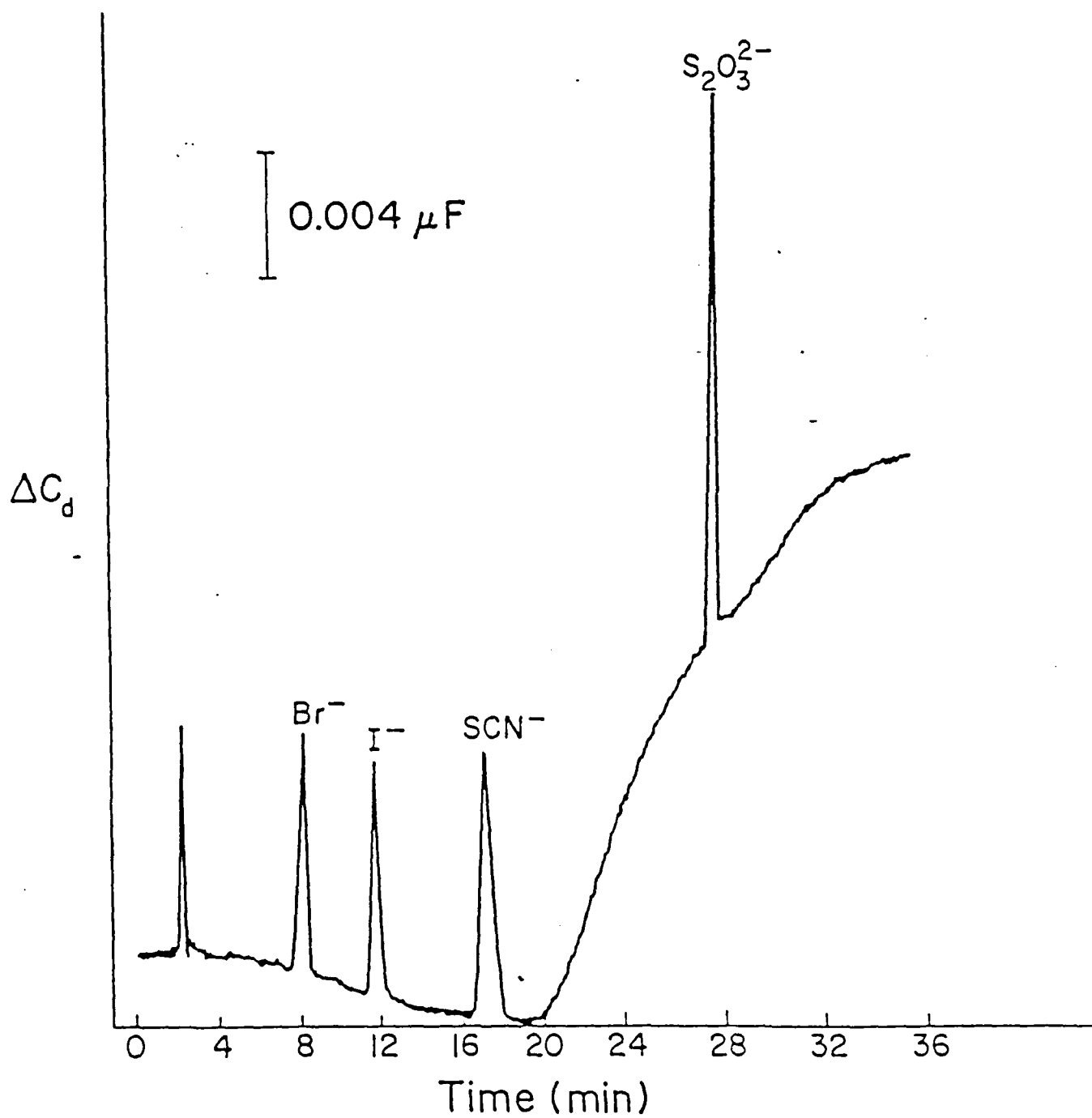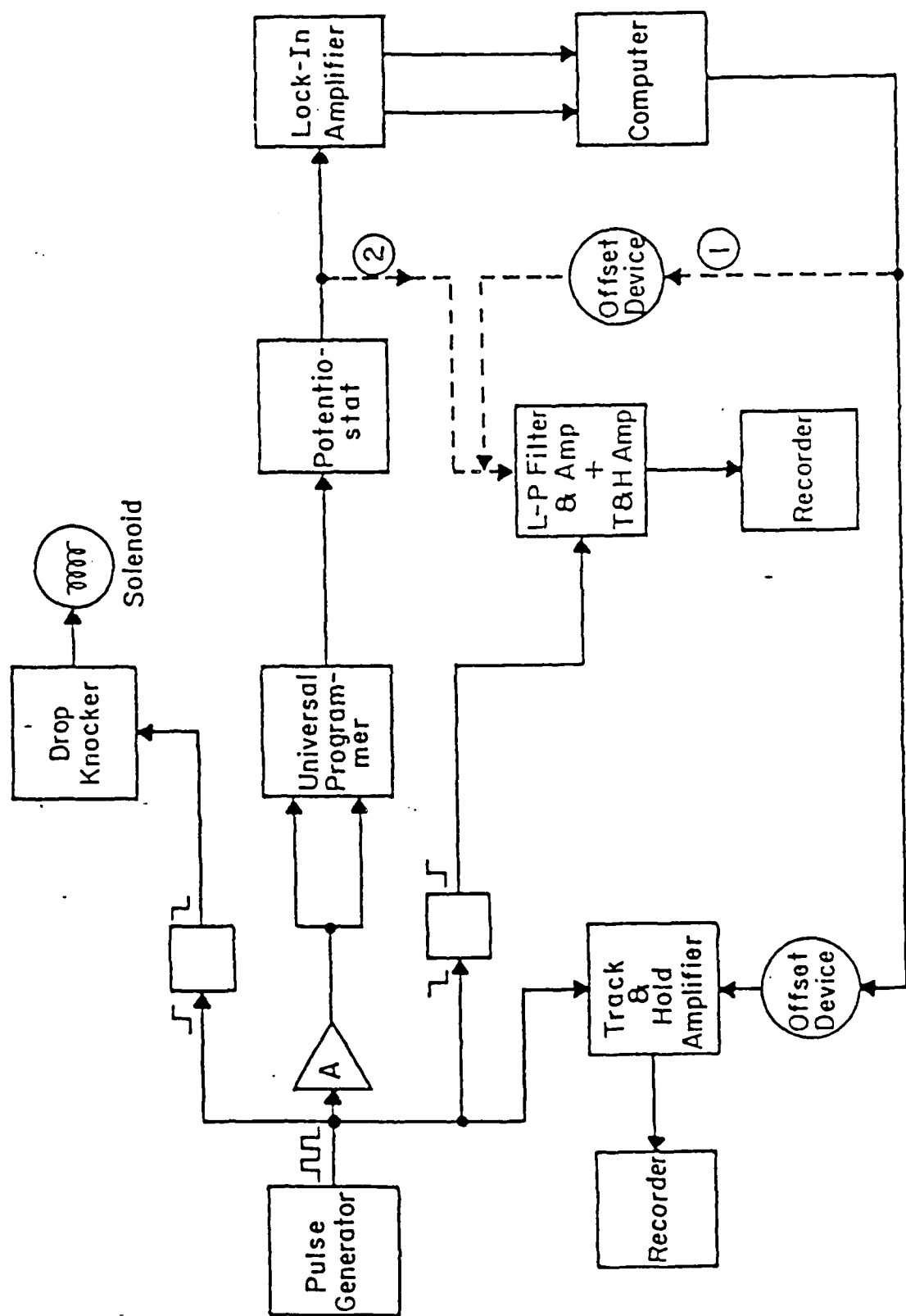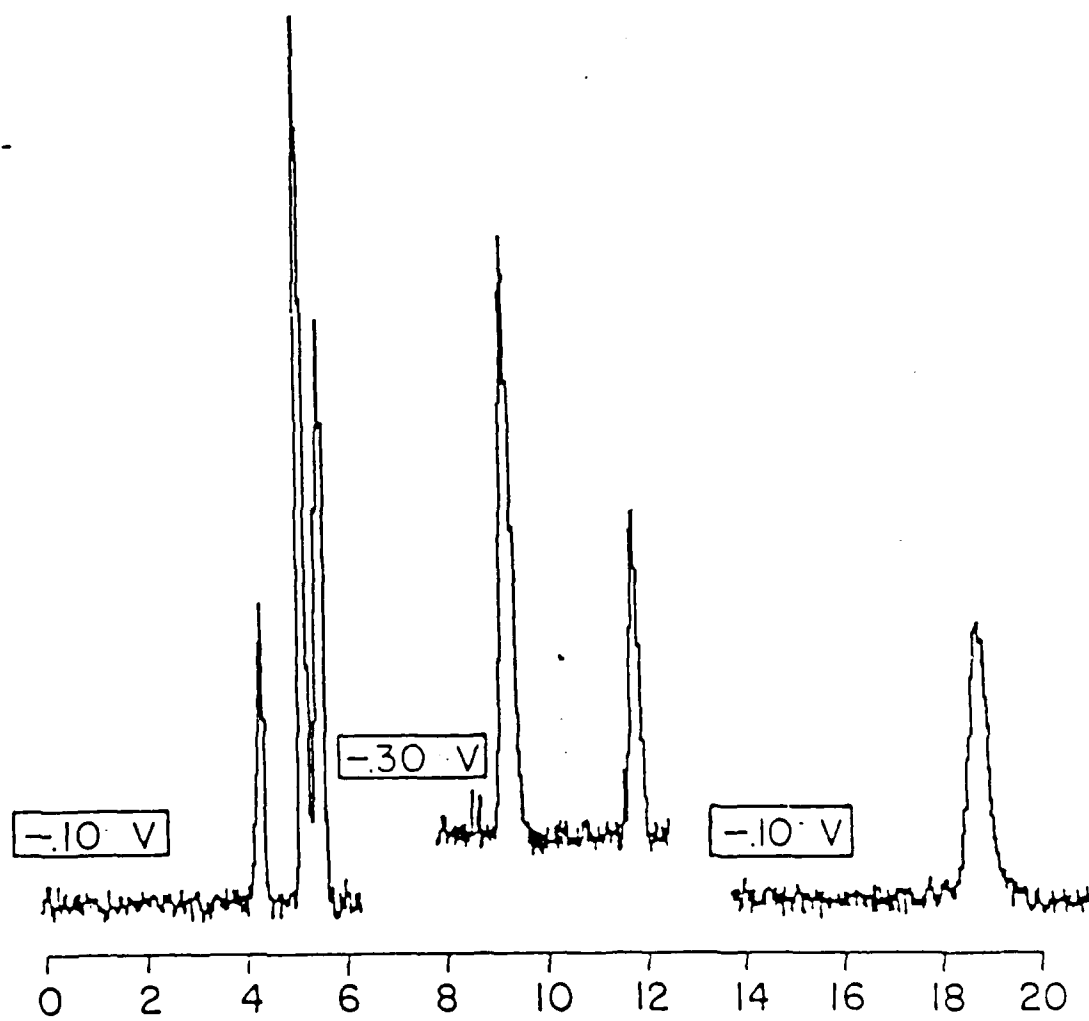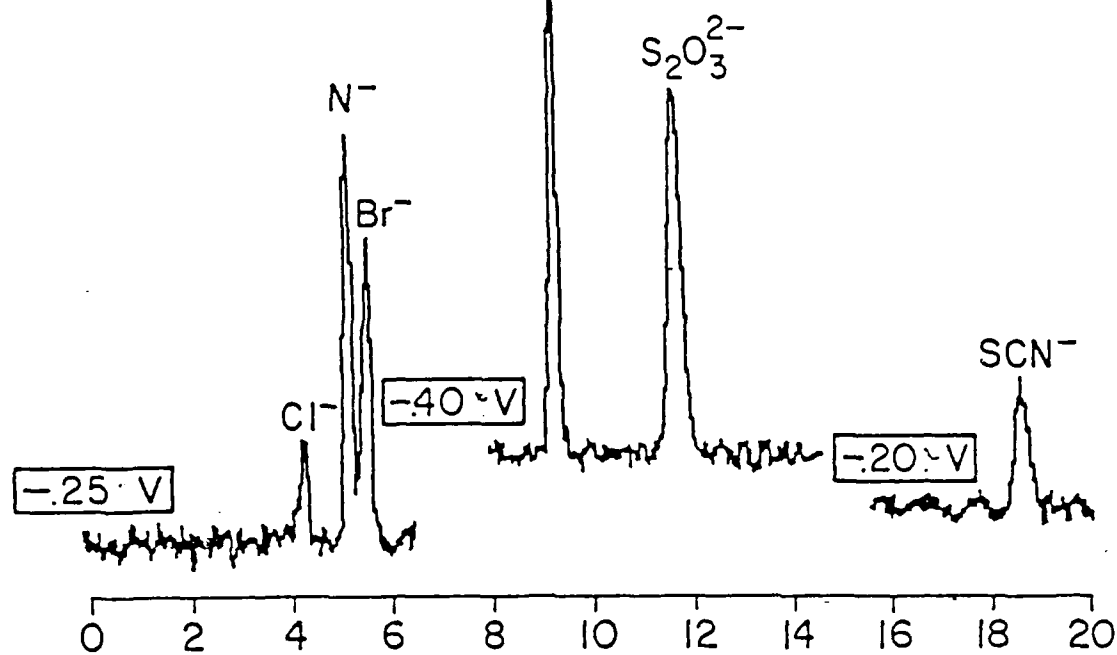
Time (min)

(a) DLC detection

Br⁻ labeled peaks: Cl⁻ and Br⁻ for traces 1 through 6

−.20 V

Time (min)

Scale markers: 0 — 6 (repeated for each of the six traces)

(b) FEC detection

Traces labeled 1 through 6

1: **−.30 V**
2: **−.20 V** Br⁻
3: **−.10 V**
4: **0.00 V** Cl⁻
5: **+.10 V** Cl⁻ Br⁻
6: **+.20 V**

Time (min)

Scale markers: 0 — 6 (repeated for each of the six traces)
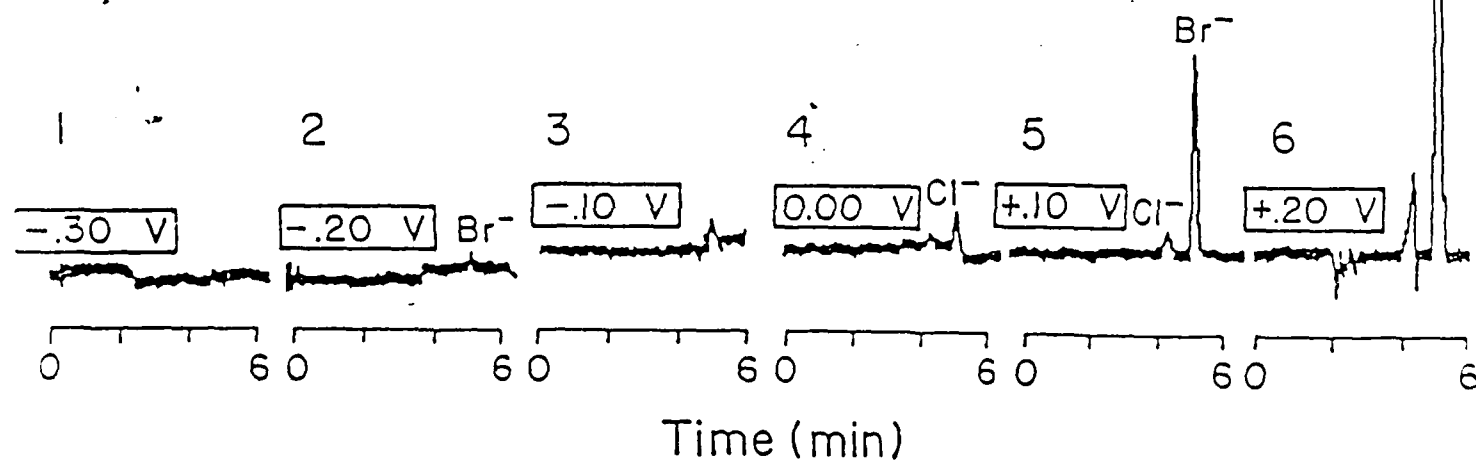
END

FILMED

MARCH, 1988

DTIC